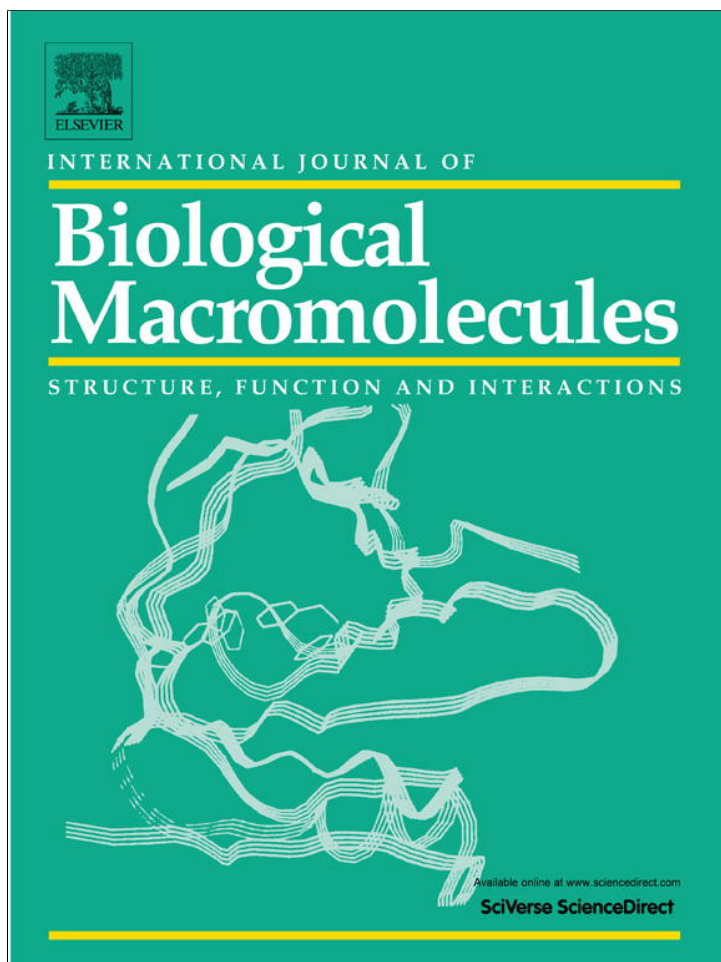


Provided for non-commercial research and education use.
Not for reproduction, distribution or commercial use.



(This is a sample cover image for this issue. The actual cover is not yet available at this time.)

This article appeared in a journal published by Elsevier. The attached copy is furnished to the author for internal non-commercial research and education use, including for instruction at the authors institution and sharing with colleagues.

Other uses, including reproduction and distribution, or selling or licensing copies, or posting to personal, institutional or third party websites are prohibited.

In most cases authors are permitted to post their version of the article (e.g. in Word or Tex form) to their personal website or institutional repository. Authors requiring further information regarding Elsevier's archiving and manuscript policies are encouraged to visit:

<http://www.elsevier.com/copyright>

Contents lists available at [SciVerse ScienceDirect](http://www.elsevier.com/locate/ijbiomac)

International Journal of Biological Macromolecules

journal homepage: www.elsevier.com/locate/ijbiomac

Vitamin E-loaded silk fibroin nanofibrous mats fabricated by green process for skin care application



Xiaoyue Sheng^a, Linpeng Fan^a, Chuanglong He^{a,b,c}, Kuihua Zhang^{a,d}, Xiumei Mo^{a,b,c}, Hongsheng Wang^{a,b,c,*}

^a Biomaterials and Tissue Engineering Lab, College of Chemistry, Chemical Engineering and Biotechnology, Donghua University, Shanghai 201620, PR China

^b State Key Laboratory for Modification of Chemical Fibers and Polymer Materials, Donghua University, Shanghai 201620, PR China

^c Key Laboratory of Textile Science & Technology, Ministry of Education, Donghua University, Shanghai 201620, PR China

^d College of Biological Engineering and Chemical Engineering, Jiaxing College, Zhejiang 314001, PR China

ARTICLE INFO

Article history:

Received 22 November 2012

Received in revised form 23 January 2013

Accepted 24 January 2013

Available online xxx

Keywords:

Silk fibroin

Vitamin E TPGS

Nanofiber

Skin care

Green process

Electrospinning

ABSTRACT

In the present study, we reported fabrication and skin benefit of a novel vitamin E (VE)-loaded silk fibroin (SF) nanofibrous mats. *RRR*- α -Tocopherol polyethylene glycol 1000 succinate (VE TPGS), a water-soluble derivative of VE, was incorporated into SF nanofiber successfully by aqua solution electrospinning for the first time. Morphology of the composite nanofibers changed with the different amount of VE TPGS: a ribbon-like shape for lower loading dose of VE TPGS, while a round shape for higher loading dose (more than 4% (wt/wt) based on the weight of SF). After treated with 75% (v/v) ethanol vapor, the composite nanofibrous mats showed an excellent water-resistant ability. *In vitro* study disclosed a sustained release behavior of VE TPGS disassociated from the nanofibrous mats. The mouse skin fibroblasts (L929 cells) cultured on the VE-loaded SF nanofibrous mats spread and proliferated much better than on cover slips. Moreover, the incorporation of VE TPGS was found strengthening the ability of SF nanofibrous mats on protecting the cells against oxidation stress induced by *tert*-butyl hydroperoxide. Our data presented impressive skin benefits of this VE-loaded SF nanofibrous mats, suggesting a promising applicative potential of this novel product on personal skin care, tissue regeneration and other related area.

© 2013 Elsevier B.V. All rights reserved.

1. Introduction

Interfacing with the environment, the skin is a target organ for pollution, ultraviolet radiation and other damage, which lead to skin aging and disorders. α -tocopherol (Vitamin E, VE) is demonstrated to have a dual role as an antioxidant and a stabilizing agent in biological membranes [1]. Whether taken orally or topically, studies suggested that VE has anti-tumorigenic, photoprotective, and skin barrier stabilizing properties, which makes VE a commonly used ingredient for skin care products [2]. While almost all forms of VE are fat-soluble, and require the presence of bile salts for absorption, some researchers suggested that a water-soluble form of VE is a better option for individuals who have difficulties in absorbing fat-soluble VE forms [3,4]. *RRR*- α -Tocopherol polyethylene glycol 1000 succinate (VE TPGS), a water-soluble derivative of VE, is prepared by ester linkage onto the end of α -tocopherol succinate, and has been documented

has good safety [5–8]. VE TPGS has proved to be intracellularly hydrolyzed releasing α -tocopherol after crossing cell membranes, thus finding applications in personal care and cosmetic products [6,7].

As well as VE, Silk fibroin (SF) from *Bombyx mori* is also favored by skin tissues and has been widely used as an additive to cosmetics [9–12]. SF is beneficial to biosynthesis of collagen, re-epithelializing, wound healing, and helps to alleviate atopic dermatitis and eliminate scarring [10–12]. Moreover, SF is able to maintain aqueous environment for skin, which is extremely important for skin tissues [13,14]. SF is also an excellent biopolymer with diverse properties such as good biocompatibility, blood compatibility, good oxygen and water permeability, biodegradability and minimal inflammatory reaction [15,16]. Recently, electrospun SF nanofibers have been widely applied in tissue engineering, wound healing and drug delivery [17–19]. However, few investigation reported on the benefit of SF nanofibrous mats used in the field of cosmetics. One of the obvious advantages of nanofibrous skin care product is the very small interstices and high surface area which allows nutrients to transfer to the skin tissue much more efficiently [20,21]. Therefore, we hypothesize that vitamin-loaded SF nanofibers could be more powerful for skin care and skin regeneration.

* Corresponding author at: College of Chemistry, Chemical Engineering and Biotechnology, Donghua University, 2999 North Renmin Road, Shanghai 201620, PR China. Tel.: +86 21 6779 2742; fax: +86 21 6779 2742.

E-mail address: whs@dhu.edu.cn (H. Wang).

In our previous study, we successfully fabricated vitamin C-loaded SF nanofibrous mats which showed great beneficial to skin cells [22]. Here, we reported a novel SF nanofibrous mats containing VE TPGS fabricated by the similar eco-friendly electrospinning process as used before [22,23]. The morphology and structure of nanofibrous mats were investigated using scanning electronic microscope (SEM), and the disassociation of VE from SF nanofibrous mats was determined with UV spectrophotometer. The skin benefits of the VE-loaded SF nanofibrous mats were tested using 3-[4,5-dimethylthiazol-2-yl]-2,5-diphenyl tetrazolium bromide (MTT) assay and an oxidative injury model *in vitro*. The present work provided a basis for further studies or practical appli-

cations of this novel nanofibrous mats in skin care, wound healing and skin regeneration.

2. Experimental

2.1. Materials

Cocoons of *B. mori* silkworm were kindly supplied by Jiaying Silk Co. (China). VE TPGS was purchased from Eurochem Asia Limited, each gram of VE TPGS contains VE 387 IU (260 mg), and *tert*-butyl hydroperoxide (*t*-BHP) were purchased from Sigma–Aldrich China Inc. L929 cells were provided by Institute of Biochemistry and Cell

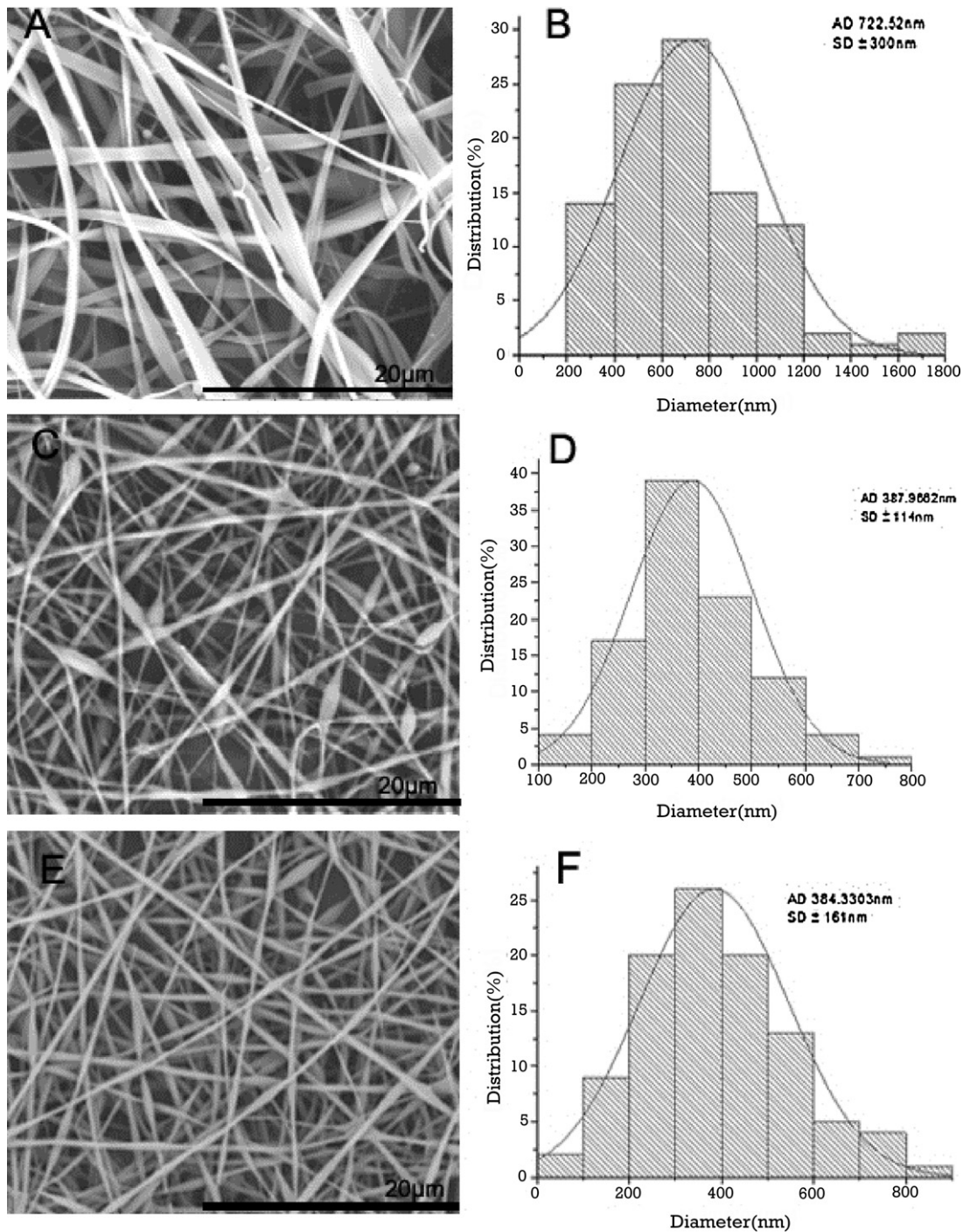


Fig. 1. SEM images (5000 \times) and diameter histograms of the VE-loaded nanofibers. A and B: SF/VE (2%); C and D: SF/VE (4%); E and F: SF/VE (8%).

Biology (Chinese Academy of Sciences, China). All other reagents involved in this study were of analysis grade or higher. Ultrapure water (Rephile Shanghai Bioscience & Technology Co., Ltd., China) was used throughout the whole study.

2.2. Preparation of regenerated SF

To remove the glue-like sericin proteins, *B. mori* silk cocoons were degummed using the sodium carbonate (0.5%, w/w) in boiling water for three times, about 30 min each. After six rinses in distilled water to remove any remaining sericin, the degummed silk fibroin was dried in a hot air oven at 45 °C and then dissolved in a ternary solvent system of CaCl₂/H₂O/CH₃CH₂OH solution (1:8:2 in molar ratio) at 65 °C for 2 h. Using cellulose tube (molecular weight cut-off 14000, Sigma–Aldrich), the fibroin–salt solution was dialyzed against deionized water at room temperature for 3 days. Then, the SF solution was filtered and lyophilized to obtain the regenerated SF (RSF) sponges.

2.3. Preparation of SF/VE TPGS composite nanofibrous mats and post-spin treatment

Heating VE TPGS at 80 °C until it was completely melted, then hydrated with hot water under continuous magnetic stirring to prepare VE TPGS aqueous solution with different concentrations, containing VE 0.5% (wt/v), 1% (wt/v) or 2% (wt/v) respectively. Stirring the mixture at room temperature for approximately 2 h, let the solution stand for 2 h, and then the regenerated SF sponges were dissolved into VE TPGS aqueous solution to render SF at the concentration of 25% (wt/v), thus the content of VE was 2% (wt/wt), 4% (wt/wt) and 8% (wt/wt) respectively based on the weight of SF. The mixture was stirred overnight to ensure complete mixing of all the contents and homogeneity of it.

The electrospinning setup used in this study consisted of a plastic syringe with a stainless steel needle (ID=0.21 mm), a syringe pump (Model 789100C, Cole-Parmer Instrument Co., USA) for controlled feed rates, an electrically grounded aluminum foil for collection, and a high voltage DC power supply (BCG6-358, BME-ICO.LTD, China). The solution was electrospun with a constant feed rate of 0.3 mL/h under positive voltage of 20 kV at a collection distance of 20 cm. To improve the crystallinity of the electrospun fibers, the collected nanofibrous mats were treated with 75% (v/v) ethanol vapor for 24 h as described before [22,23], and then dried under vacuum for 24 h at room temperature prior to use.

2.4. Characterization of the nanofibrous mats

Morphology and diameter of the electrospun nanofibers were observed with a scanning electronic microscope (SEM) (TM-1000, Hitachi, Japan) at an accelerated voltage of 10 kV. All samples were coated with 10 nm thick gold film before measurements. The average fiber diameter was determined from 100 random measurements on a typical SEM image using Image-J 1.34 software (National Institutes of Health, USA).

Fourier transform infrared attenuated total reflectance spectroscopy (FTIR-ATR) was obtained at room temperature using a FT-IR spectrophotometer (Avatar380, USA). All spectra were recorded by absorption mode at 2 cm⁻¹ interval and in the wavelength range of 4000–500 cm⁻¹ wave numbers.

X-ray diffractometry (XRD) for the nanofibers before and after post-treatment was obtained with a D/Max-2550PC diffractometer (Rigaku, Japan). The measurements were under Cu Ka1, 40 kV and 300 mA as X-ray source. XRD data was collected over a 2θ range of 5°–60°.

2.5. Drug encapsulation efficiency and release studies in vitro

Accurately wighted composite nanofibrous mats with treatment of 75% (v/v) ethanol vapor were decomposed in proteinase K solution (0.5 mg/mL in 12.5 mM Tris–HCl buffer solution, pH 8.0) at 37 °C for 3 h. After filtration through a 0.22 μm filter (RF-jet), the solution was measured at 284 nm using a UV spectrophotometer. To minimize the interference of SF, the OD₂₈₄ value of the same amount of pure SF nanofibrous mats (which was treated under the exact same conditions) was taken out from that of the samples. The actual amount of VE TPGS in the nanofibrous mats was determined from the obtained data against a predetermined calibration curve for VE TPGS. The encapsulation efficiency was then calculated as follows:

$$\text{Encapsulation efficiency (\%)} = \frac{C_a}{C_i} \times 100\%$$

where C_a is the calculated amount of the encapsulated VE TPGS and C_i is the initial amount of VE TPGS used for electrospinning.

The release of VE TPGS from SF nanofibers was carried out over a period of days *in vitro*. Samples were incubated in phosphate-buffered saline (PBS) with a continuous swing of 90 rpm at 37 °C. At a specified period between 0 and 72 h, 1 ml of the release solution was withdrawn and an equal volume of PBS was refilled. The amount of VE TPGS in the sample was determined using UV detector.

2.6. Assessment of cellular proliferation on the nanofibrous mats

L929 cells were cultured in RPMI 1640 medium (Gibco) supplemented with 10% fetal bovine serum (Gibco) and incubated in a humidified incubator at 37 °C, with 5% CO₂. The nanofibrous mats were collected on circular glass cover slips (14 mm in diameter) for cellular study. After treatment with 75% (v/v) ethanol vapor, nanofiber-deposited cover slips were placed into 24-well culture plate and fixed with autoclaved steel rings, herein, nanofiber-free cover slips as controls. L929 cells were seeded on the nanofibrous mats and nanofiber-free cover slips at the same density of 1.0 × 10⁴ cells/well. Initially, the volume of cells and medium was 400 μL for each well, and then 200 μL of fresh medium was added to each well every 3 days. L929 cells were allowed to proliferate on the nanofibrous mats and cover slips for 1, 3, 5 and 7 days. At these specific time point, cell-seeded or unseeded nanofibrous mats and cover

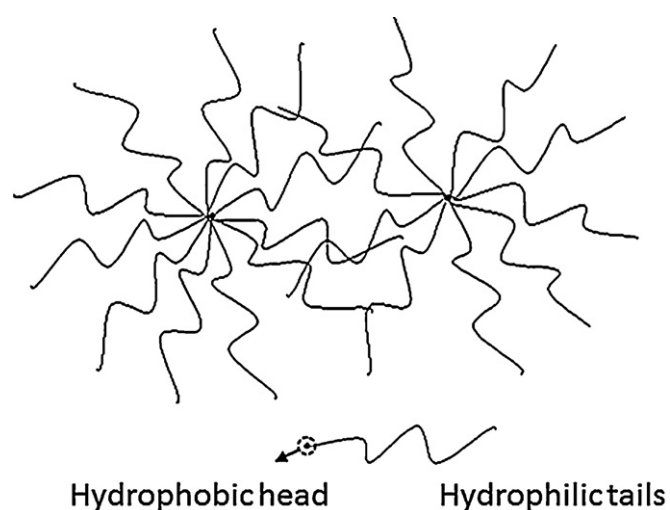


Fig. 2. Schematic representation of polymer–micelle complex formed from the surfactant of VE TPGS polymer due to the long hydrophilic tails tangle and associate with each other.

slips were rinsed with PBS for three times following medium being removed. Thereafter, each well was supplemented with 400 μ L of serum-free Dulbecco's modified Eagle's medium (DMEM) (Gibco) containing 0.5 mg/ml MTT (Sigma–Aldrich). After being cultured for 4 h, the medium was completely aspirated and the formazan formed was dissolved in 400 μ L of dimethylsulfoxide. Then 100 μ L of the solution was withdrawn to measure the absorption at 492 nm with a microplate reader (Multiskan MK3; Thermo Labsystems Co., China), and the background value of cell-unseeded nanofibrous mats or cover slips was taken out correspondingly.

2.7. Morphology observation of cultured cells on the nanofibrous mats

Cells were seeded on the nanofibrous mats as described above. At day 3, culture medium was discarded, the content was washed

with PBS and then fixed with 4% paraformaldehyde for 40 min at room temperature. After being rinsed with PBS for several times, the fixed samples were dehydrated with graded ethanol for 8 min each, then dried overnight and observed under SEM (S-2700, Hitachi, Japan) at a voltage of 15 kV following being sputter-coated with a gold film.

2.8. Antioxidation assay

L929 cells were seeded on nanofibrous mats as described above and exposed to different concentrations of *t*-BHP (0, 50, 100, 200 and 400 μ M) for 24 h when their confluences were about 90%. Then, *t*-BHP was removed and the wells were rinsed with PBS twice. After that, cell viability was quantified by MTT assay as described above.

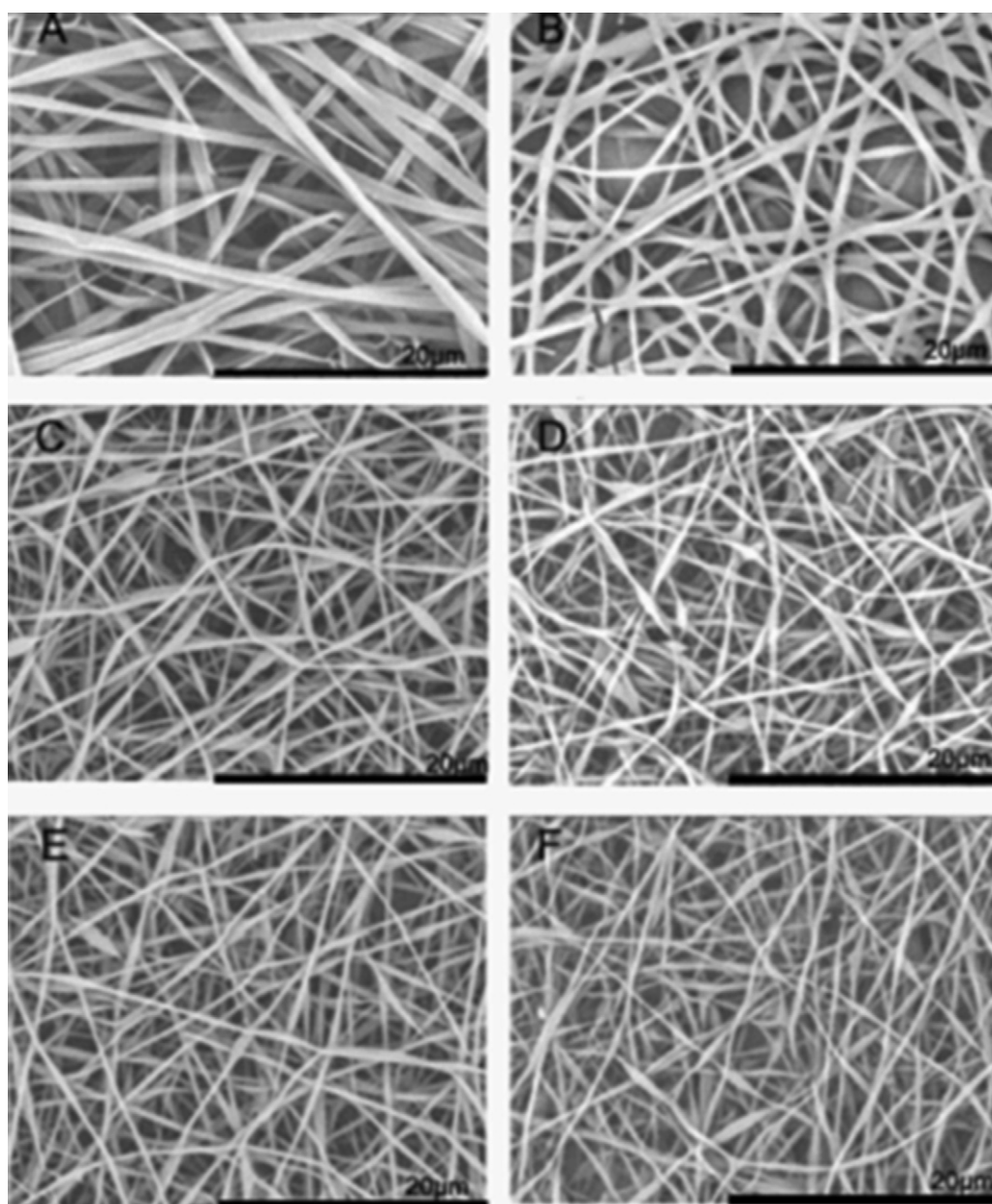


Fig. 3. SEM images of as-spun SF nanofibrous mats treated with 75% (v/v) ethanol vapor. A and B: SF/VE (2%); C and D: SF/VE (4%); E and F: SF/VE (8%); A, C and E: After treatment with 75% (v/v) ethanol vapor for 24 h; B, D and F: after treatment with 75% (v/v) ethanol vapor for 24 h and then soaking in PBS for 4 days.

2.9. Statistical analysis

All experiments were conducted at least three times and data were reported as mean \pm standard deviation (SD). Statistical analysis was performed using Student's *t*-test. In all statistical comparisons, a *P*-value of less than 0.05 was considered statistically significant. The error bars in the figures are the SD of the data.

3. Results and discussion

3.1. Morphology of the nanofibrous mats

According to our previous study [22,23], the electrospinning concentration of SF was fixed as 25% (wt/v) in this work, while the amounts of VE were 2% (wt/wt), 4% (wt/wt) and 8% (wt/wt) respectively based on the weight of SF, and the outputs were denoted as SF/VE (2%), SF/VE (4%) and SF/VE (8%) respectively. As shown in Fig. 1, the morphology of the nanofibers changed with the different amount of VE TPGS: ribbon-like fibers resulted from SF/VE (2%), similar with the pure SF nanofibers previously reported [22,23];

while for SF/VE (4%) and SF/VE (8%), round and smooth fibers resulted from, a few beaded structure also displayed.

Owing a big lipophilic tail (polyethylene glycol) and a hydrophobic head (tocopherol succinate), VE TPGS can form micelles in water above its critical micelle concentration (0.02%) [24]. The hydrophobic head groups are located in the core of the micelle and the hydrophilic tails are directed outward in contact with water (Fig. 2). The polymer-micelle complex forming due to the long hydrophilic tails tangle and associate with each other (Fig. 2), together with the intermolecular hydrogen bonds between SF and PEG, endows the solution an apparent viscosity. In this work, the addition of VE TPGS did result in higher viscosity which favors the electrospinnability and the formation of smooth fibers. On other side, higher solution viscosity may also resulted in the formation of some beaded structure, as the solution become a bit difficult to force through the syringe needle and make the control of the solution flow rate unstable [25,26].

In order to improve its water-resistance, the electrospun nanofibrous mats were treated with 75% (v/v) ethanol vapor as described before [22,23]. After treated with 75% (v/v) ethanol vapor, the water-resistance of the nanofibrous mats were dramatically increased, so that the structure of the mats still kept intact after being soaked in the PBS for 4 days (Fig. 3B, D and F).

3.2. Secondary structure of the nanofibrous mats

FT-IR spectroscopy has sufficient sensitivity to examine the structure of proteins [27]. The FTIR spectra of VE TPGS-loaded nanofibers bore a close similarity to pure SF nanofibers. The characteristic absorption bands at 1650–1660 (amide I), 1535–1545 (amide II), 1235 (amide III) and 669 cm^{-1} (amide V), attributed to the SF with random coil or α -helix conformation (silk I), and the characteristic absorption bands at 1625–1640, 1515–1525, 1265 and 696 cm^{-1} , attributed to the SF with β -sheet structure conformation (silk II) [28]. Our data showed after the treatment with 75% (v/v) ethanol vapor, the nanofiber's absorption peaks appeared at 1651 (amide I), 1537 (amide II) and 1240 cm^{-1} (amide III) shifted to 1630, 1520, 1236 cm^{-1} , indicating a conformation change from silk I to silk II (Fig. 4).

X-ray diffraction was also carried out to study the crystalline structure of the nanofibers. The 2θ peaks belonged to silk I and silk II of SF had been summarized by Chen et al. [29]. Before the

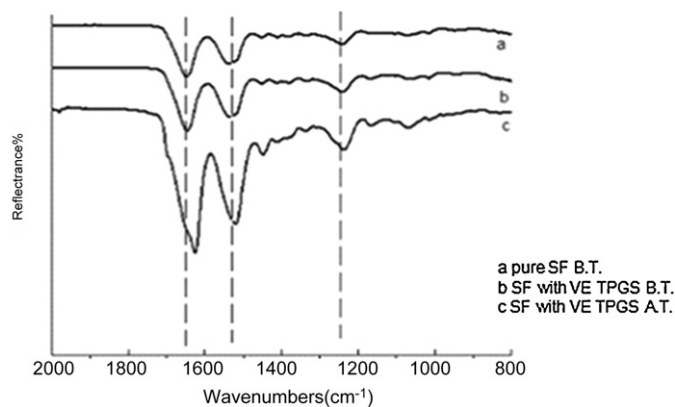


Fig. 4. ATR-FTIR transmission spectra of the nanofibers before or after post-treatment (B.T.: before post-treatment; A.T.: after post-treatment).

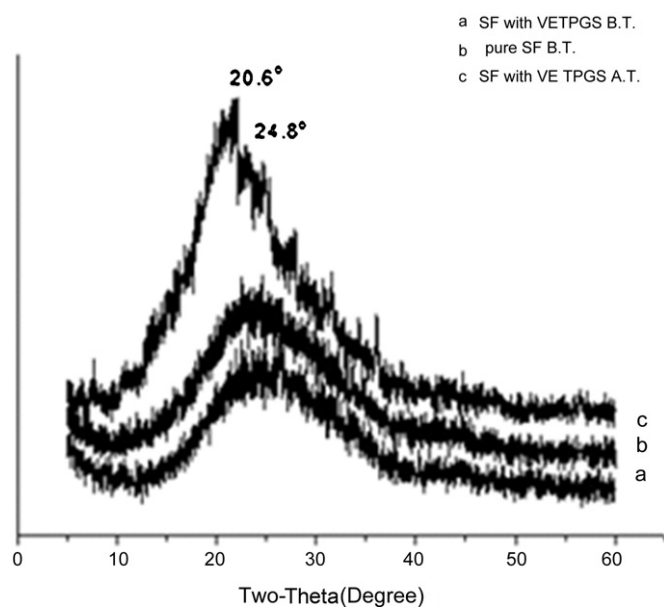


Fig. 5. Wide-angle X-ray diffraction profiles of SF vitamin-loaded nanofibers (B.T.: before post-treatment; A.T.: after post-treatment).

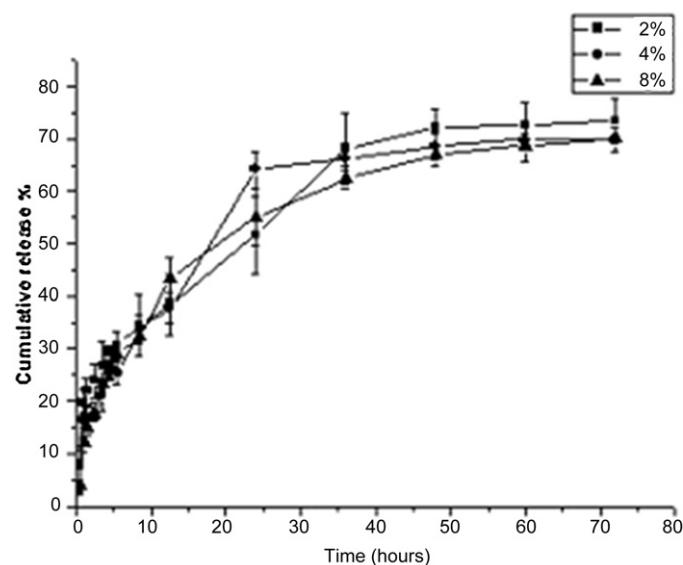


Fig. 6. *In vitro* release of VE from SF nanofibrous mats containing different amounts of VE.

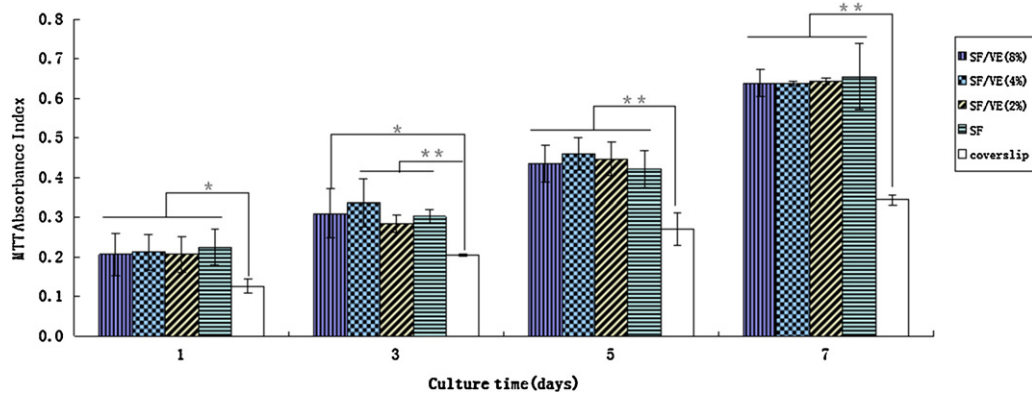


Fig. 7. The viability of cells grown on the coverslips or different SF nanofibrous substrates at days 1, 3, 5 and 7 (* $P < 0.05$, ** $P < 0.01$).

post-treatment, both pure SF nanofibers and VE-loaded SF nanofibers showed no obvious 2θ peak, which refers to conformation of random coil. As shown in Fig. 5, after treated with 75% (v/v) ethanol vapor, the VE-loaded nanofibers exhibited 2θ peaks at 20.6°

and 24.8° , which belonged to β crystal (silk II), consistent with the results of FTIR analysis. Our results indicated that it's not VE TPGS but post-treatment transformed crystal structure of SF from silk I (water-soluble) to silk II (water-insoluble).

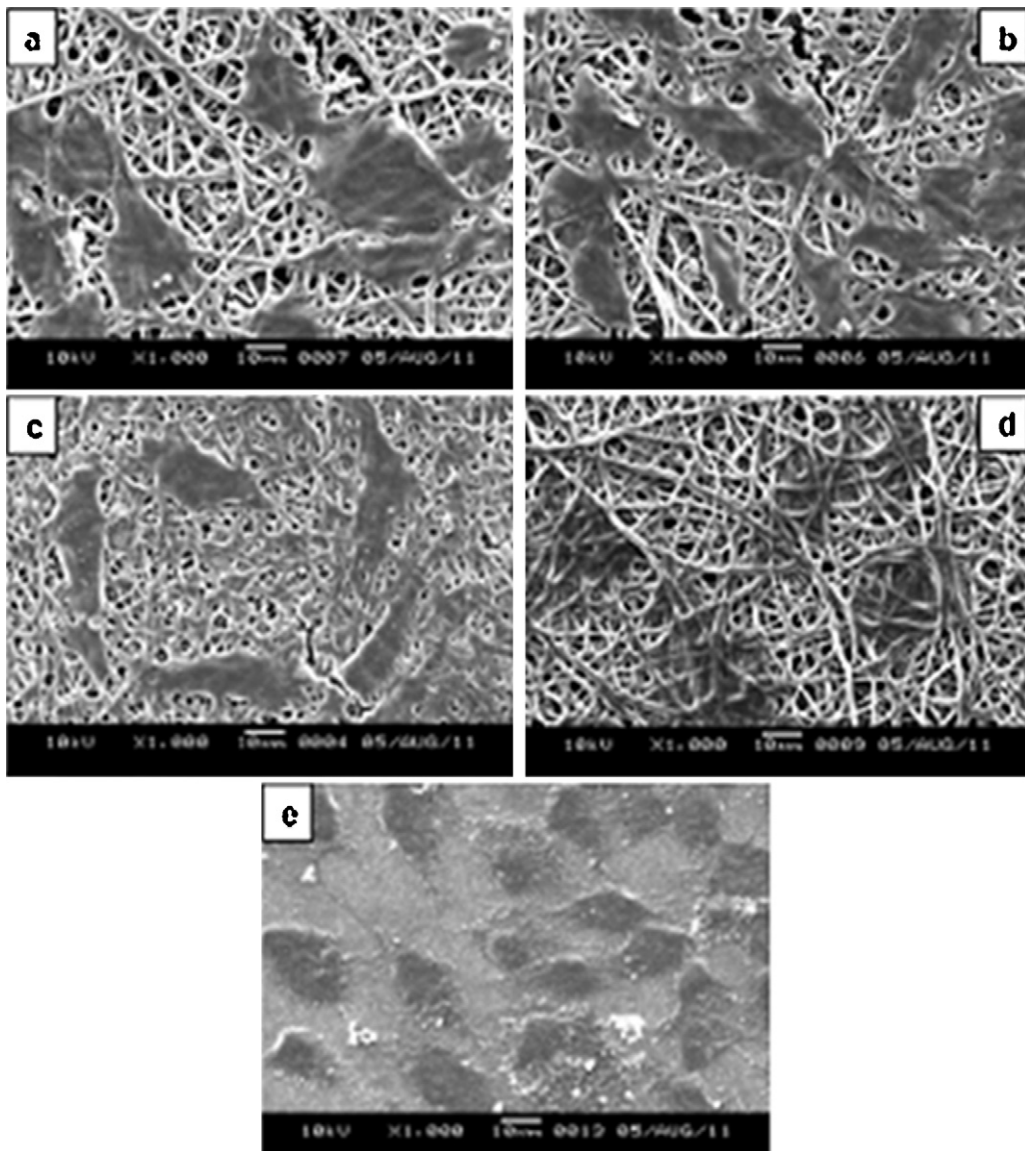


Fig. 8. SEM images (1000 \times) illuminate the morphology of L929 cells grown on the nanofibrous mats and coverslips (a: SF/VE (2%); b: SF/VE (4%); c: SF/VE (8%); d: pure SF; e: cover slips).

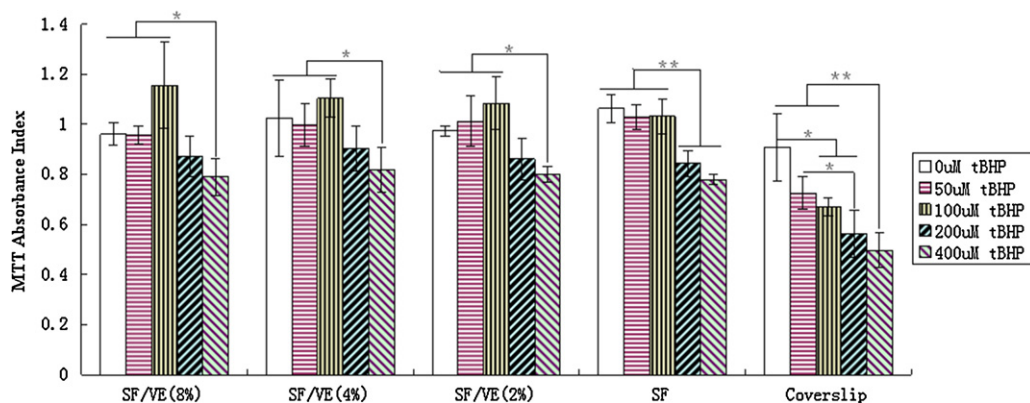


Fig. 9. the viability of L929 cells cultured on different substrates exposure to *t*-BHP of different concentrations (* $P < 0.05$, ** $P < 0.01$).

3.3. In vitro release of VE TPGS from the nanofibrous mats

The actual amount of the VE in the nanofibrous mats was determined prior to their release studies. The encapsulation efficiency of VE was calculated to be 65.82%, 78.59% and 70.02% according to the nanofibrous mats of SF/VE (2%), SF/VE (4%) and SF/VE (8%) respectively. No obvious differences were observed in the release characteristics between the three drug-loaded nanofibrous mats, they all exhibited a slightly burst release of VE TPGS during the first 30 min (reached a plateau at about 7%), followed by a slow release over 72 h (Fig. 6). It is known that the release mechanism of the drug release behavior could be divided into: (1) diffusion, (2) polymer erosion and (3) combination of diffusion and polymer erosion [30]. After post-treatment, SF is demonstrated to be barely degradable over months [31,32], so diffusion could be mainly responsible for the drug release. VE TPGS has both hydrophobic group (α -tocopherol succinate) and hydrophilic group (PEG), which can help the formation of hydrophobic–hydrophilic micro domain structure and led to intermicellar interaction. Moreover, the PEG group may be hydrogen-bonded to the amide group of SF. These two properties probably lead to the sustained release behavior of VE TPGS from the SF nanofiber.

3.4. Morphology and proliferation of L929 cells cultured on the nanofibrous mats

The proliferation of L929 cells grown on the SF nanofibrous mats was analyzed by MTT assay at days 1, 3, 5 and 7. As shown in Fig. 7, the cell population increased obviously from days 1–7. Both pure and VE-loaded SF nanofibrous mats showed a better ability on encouraging the cells proliferation than the cover slips. To further investigate the cell compatibility of the nanofibrous mats, the morphology of the cells grown on the mats were observed by SEM. Cells on the nanofibrous mats presented a fusiform morphology spreading largely and bridging each other (Fig. 8a–d). While cells on the cover slips appeared very differently: they adopted a polygonal morphology without obvious spreading (Fig. 8e). Cells cultured on the nanofibrous matrices spread to bridge each other could be beneficial to the cell–cell and cell–matrix signal transduction and in turn greatly encouraged cell proliferation [11], which may explain the above results of cell viability determined by MTT assay. Our data demonstrated that the addition of VE TPGS has no adverse effect on the good cell compatibility of SF.

3.5. The viability of L929 cells cultured on the nanofibrous mats under oxidative stress

To further explore the skin benefits of the VE-loaded SF nanofibrous mats, their antioxidant capability was investigated using

the *t*-BHP-induced oxidative injury model. The *t*-BHP is a potent oxidant and demonstrated to promote the generation of reactive oxygen species (ROS) which greatly damage cells [33]. As shown in Fig. 9, our data showed that the viability of the cells cultured on cover slips was significantly affected by *t*-BHP, even at lower concentration; while for the cells on the pure SF nanofibrous mats, significant decrease of viability was found on higher concentration of *t*-BHP (more than 200 μ M); and the viability of the cells on the VE-loaded SF nanofibrous mats did not significantly decreased till the *t*-BHP concentration up to 400 μ M. Our data indicated that SF nanofibrous mats has great benefit to cells against oxidative stress and such benefit can be strengthened by the incorporation of VE TPGS. It has been reported that VE TPGS is more effective at eliminating ROS than α -tocopherol succinate [34]. Here, our data confirmed the remarkable antioxidative capacity of VE TPGS. Our work suggested the VE TPGS-loaded SF nanofibrous mats a promising applicative potential in skin care, tissue regeneration as well as anticancer since it can effectively protect cells against damage from ROS.

4. Conclusion

In summary, through an eco-friendly process, we successfully fabricated a novel VE TPGS-loaded SF nanofibrous mats which well inherited the excellent characteristics of skin benefit of both SF and VE, encouraging the proliferation of skin fibroblasts and enhancing the survival of the cells against oxidative stress. Our data indicated that the incorporation of VE TPGS significantly strengthen the excellent skin benefits of SF nanofiber, implying a promising application of VE TPGS-loaded SF nanofibrous mats in personal skin care, tissue regeneration and other related area.

Acknowledgements

This research was supported by the Shanghai–Unilever Research and Development Fund (08520750100), the Natural Science Foundation of Shanghai (12ZR1400300), National Nature Science Foundation of China (31070871, 31271028), Fundamental Research Funds for the Central Universities and Open Foundation of State Key Laboratory for Modification of Chemical Fibers and Polymer Materials (LK1111).

References

- [1] J.S. Trivedi, S.L. Krill, J.J. Fort, European Journal of Pharmacology Science 3 (1995) 241–243.
- [2] J.J. Thiele, S. Ekanayake-Mudiyanselage, Molecular Aspects of Medicine 28 (2007) 646–667.
- [3] R.J. Sokol, J.E. Heubi, N. Butler-Simon, H.J. McClung, J.R. Lilly, A. Silverman, Gastroenterology 93 (1987) 975–985.

- [4] M.G. Traber, H.J. Kayden, J.B. Green, M.H. Green, *American Journal of Clinical Nutrition* 44 (1986) 914–923.
- [5] S. Somavarapu, S. Pandit, G. Gradassi, M. Bandera, E. Ravichandran, O.H. Alpar, *International Journal of Pharmaceutics* 298 (2005) 334–337.
- [6] O. Aydemir, S. Celebi, T. Yilmaz, H. Yekeler, A.S. Kükner, *International Ophthalmology* 25 (2004) 283–289.
- [7] M.G. Traber, C.A. Thellman, M.J. Rindler, H.J. Kayden, *American Journal of Clinical Nutrition* 48 (1988) 605–611.
- [8] W.J. Krasavage, C.J. Terhaar, *Journal of Agricultural and Food Chemistry* 25 (1977) 273–278.
- [9] C. Sobajo, F. Behzad, X.F. Yuan, A. Bayat, *Eplasty* 8 (2008) 438–446.
- [10] A. Sugihara, *Proceedings of the Society for Experimental Biology and Medicine* 225 (2000) 58–64.
- [11] D.H. Roh, *Journal of Materials Science: Materials in Medicine* 17 (2006) 547–552.
- [12] G. Ricci, A. Patrizi, B. Bendandi, G. Menna, E. Varotti, M. Masi, *British Journal of Dermatology* 150 (2004) 127–131.
- [13] Z.D. Draelos, *Current Problems in Dermatology* 12 (2000) 235–239.
- [14] A.V. Daithankar, M.N. Padamwar, S.S. Pisal, A.R. Paradkar, K.R. Mahadik, *Indian Journal of Biotechnology* 4 (2005) 115–121.
- [15] C. Vepari, D.L. Kaplan, *Progress in Polymer Science* 32 (2007) 991–1007.
- [16] W.H. Park, L. Jeong, D.I. Yoo, S. Hudson, *Polymer* 45 (2004) 7151–7157.
- [17] N. Bhardwaj, S.C. Kundu, *Biotechnology Advances* 28 (2010) 325–347.
- [18] D. Liang, B.S. Hsiao, B. Chu, *Advanced Drug Delivery Reviews* 59 (2007) 1392–1412.
- [19] P. Lu, B. Ding, *Recent Patents on Nanotechnology* 2 (2008) 169–182.
- [20] *Electrospun pharmaceutical compositions*, USA, 2001, PCT/US01/02399.
- [21] Z.M. Huang, Y.Z. Zhang, M. Kotaki, S. Ramakrishna, *Composites Science and Technology* 63 (2003) 2223–2253.
- [22] L.P. Fan, H.S. Wang, K.H. Zhang, Z.X. Cai, C.L. He, X.Y. Sheng, X.M. Mo, *RSC Advances* 2 (2012) 4110–4119.
- [23] L.P. Fan, H.S. Wang, K.H. Zhang, C.L. He, Z.X. Cai, X.M. Mo, *Journal of Biomaterials Science* 23 (2012) 497–508.
- [24] R. Nagarajan, C. Drew, C.M. Mello, *Journal of Physical Chemistry C* 111 (2007) 16105–16108.
- [25] J.M. Deitzel, J. Kleinmeyer, D. Harris, N.C. Beck Tan, *Polymer* 42 (2001) 261–272.
- [26] Q.P. Pham, U. Sharma, A.G. Mikos, *Tissue Engineering* 12 (2006) 1197–1211.
- [27] G. Steiner, S. Tunc, M. Maitz, R. Salzer, *Analytical Chemistry* 79 (2007) 1311–1316.
- [28] J. Magoshi, M. Mizuide, Y. Magoshi, *Journal of Polymer Physical Edition* 17 (1979) 515–520.
- [29] X. Chen, W.J. Li, T.Y. Yu, *Journal of Polymer Science Part B: Polymer Physics* 35 (1997) 2293–2296.
- [30] Y.C. Dong, Z.P. Zhang, S.S. Feng, *International Journal of Pharmaceutics* 350 (2008) 166–171.
- [31] R.E. Unger, M. Wolf, K. Peters, A. Motta, C. Migliaresi, C. James Kirkpatrick, *Biomaterials* 25 (2004) 1069–1075.
- [32] K.H. Zhang, A.L. Yin, C. Huang, *Polymer Degradation and Stability* 96 (2011) 2266–2275.
- [33] P. Kovacic, R. Somanathan, *Reviews of Environmental Contamination and Toxicology* 203 (2010) 119–138.
- [34] H.J. Youk, E. Lee, *Journal of Controlled Release* 107 (2005) 43–52.